Interaction between γC87 and γR242 residues participates in energy coupling between catalysis and proton translocation in *Escherichia coli* ATP synthase

Yunxiang Li [a,b,*], Xinyou Ma [c] and Joachim Weber [b,d]

[a] Department of Chemistry and Biochemistry, Texas Woman's University, Denton, TX 76204, USA; [b] Department of Chemistry and Biochemistry, Texas Tech University, Lubbock, TX 79409, USA;

[c] Department of Chemistry, The University of Chicago, Chicago, IL 60637, USA; [d] The Center for Membrane Protein Research, Texas Tech University Health Sciences Center, Lubbock, TX 79430, USA

Abstract

Functioning as a nanomotor, ATP synthase plays a vital role in the cellular energy metabolism. Interactions at the rotor and stator interface are critical to the energy transmission in ATP synthase. From mutational studies, we found that the γC87K mutation impairs energy coupling between proton translocation and nucleotide synthesis/hydrolysis. An additional glutamine mutation at γR242 (γR242Q) can restore efficient energy coupling to the γC87K mutant. Arrhenius plots and molecular dynamics simulations suggest that an extra hydrogen bond could form between the side chains of γC87K and β_{TP}E381 in the γC87K mutant, thus impeding the free rotation of the rotor complex. In the enzyme with γC87K/γR242Q double mutations, the polar moiety of γR242Q side chain can form a hydrogen bond with γC87K, so that the amine group in the side chain of γC87K will not hydrogen-bond with β_E381. As a conclusion, the intra-subunit interaction between positions γC87 and γR242 modulates the energy transmission in ATP synthase. This study should provide more information of residue interactions at the rotor and stator interface in order to further elucidate the energetic mechanism of ATP synthase.

Terminology

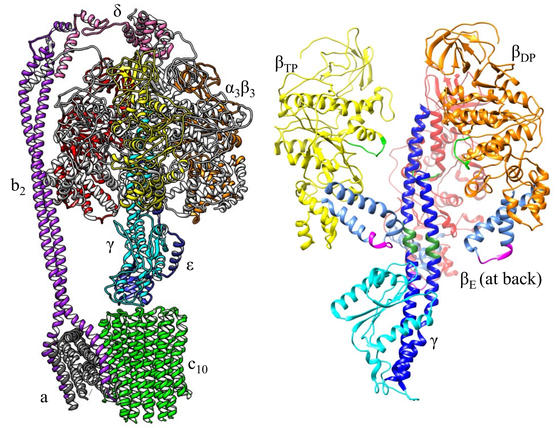

Fig. 1 Subunit structure, domains and motifs in ATP synthase. The figure was created using Chimera based on a cryo-EM structure of *E. coli* ATP synthase (PDB ID: 5T4O). (A) The holoenzyme of *E. coli* ATP synthase requires proper assembly of two subcomplexes: a membrane-bound portion F_o and a water soluble portion F_1. A molecule of F_o complex is comprised of one copy of subunit a (gray), two b subunits (purple) and ten c subunits (green, the c-ring). The F_1 complex consists of the $\alpha_3\beta_3$ catalytic hexamer (the three α subunits are colored white, and three β subunits are colored red, orange and yellow respectively), γ subunit (cyan), δ subunit (pink) and ε subunit (blue). (B) β_E, β_{DP} and β_{TP} subunits are colored in red, orange and yellow respectively. Within each β subunit, the upper β catch loop (βY297-D305) is shown in light green, and the helix-turn-helix lever domain (called the "DELSEED-loop") is shown in light blue, with the DELSEED motif itself in magenta. The γ subunit contains a coiled-coil domain (dark blue) and a globular "foot" domain (cyan). The green helixes (γ T20-M25 and M246-N252) located at the middle of γ are named the γ "neck" area.

CCCP: carbonyl cyanide *m*-chlorophenylhydrazone.

ATP: Adenosine triphosphate.

Results

1. Mutation γC87K causes inefficient energy coupling in ATP synthase, but mutation γR242Q can suppress the energy uncoupling in the γC87K mutant.

Table 1
Energy coupling properties of γC87 mutants.

Strain	Growth yield	ATP synthase amount	ATPase activity	ATP-driven H^+ pumping	NADH-driven H^+ pumping
	%	%	unit/mg protein	%	%
WT	100	100	4.6 (0.8)	100	100
γC87A	95 (2)	90 (10)	3.9 (0.2)	88 (5)	90 (5)
γC87D	92 (3)	90 (10)	5.7 (0.3)	101 (3)	ND
γC87E	84 (3)	130 (20)	7.5 (0.4)	92 (4)	ND
γC87F	74 (4)	90 (10)	5.1 (0.4)	73 (5)	ND
γC87K	17 (2)	80 (10)	2.8 (0.5)	6 (3)	75 (6)
pUC18	< 1	0	< 0.01	< 1	99 (1)

Table 2
Suppressor mutations at γR242 restore energy coupling in ATP synthase.

Strain	Growth yield		ATP synthase amount	ATPase activity	ATP-driven H^+ pumping	NADH-driven H^+ pumping
	30 °C %	37 °C %	%	unit/mg protein	%	%
WT	100	100	100	4.6 (0.8)	100	100
γC87K	17 (2)	8 (1)	80 (10)	2.8 (0.5)	6 (3)	75 (6)
γR242A	86 (4)	97 (3)	110 (10)	4.9 (0.5)	76 (5)	84 (3)
γR242C	95 (3)	98 (4)	110 (20)	2.4 (0.4)	87 (4)	95 (3)
γR242E	66 (4)	30 (3)	100 (10)	2.3 (0.4)	48 (4)	94 (3)
γR242L	81 (2)	85 (4)	100 (10)	2.4 (0.2)	56 (5)	85 (4)
γR242S	99 (2)	97 (4)	100 (10)	2.5 (0.3)	88 (4)	97 (2)
γC87K/γR242A	75 (4)	23 (4)	110 (10)	4.0 (0.6)	30 (3)	84 (3)
γC87K/γR242C	72 (3)	35 (3)	110 (20)	3.1 (0.4)	32 (4)	85 (5)
γC87K/γR242E	33 (4)	8 (2)	70 (10)	1.6 (0.2)	8 (2)	90 (3)
γC87K/γR242L	31 (3)	7 (2)	80 (10)	1.7 (0.2)	3 (2)	92 (3)
γC87K/γR242Q	85 (4)	90 (5)	110 (10)	4.5 (0.7)	52 (4)	80 (5)
γC87K/γR242S	73 (3)	22 (4)	110 (10)	4.0 (0.5)	45 (5)	72 (6)

Table 1 and 2. DK8 strain expressing WT, mutant or no ATP synthase was allowed to grow in 8 mM succinate medium at 30 °C or 37 °C until saturation. Growth yield was quantified from the turbidity of cell culture by measuring absorbance at 590 nm. The membrane-bound ATP synthase amount was measured by Western Blot using anti-γ antibody. ATPase activities were determined by the amount of inorganic phosphate released at 37 °C. To evaluate proton pumping ability of ATP synthase, inverted cell membrane vesicles were suspended in proton pumping buffer. Either 1 mM ATP or 2 mM NADH was added to initiate proton pumping across membrane. Acridine orange fluorescence intensities were monitored at emission wavelength 530 nm with excitation wavelength at 460 nm. 5 μM CCCP was added to terminate the reaction and to establish 100% fluorescence intensity. All percentage values in this table are normalized against WT. Standard deviations are shown in parenthesis. ND, not determined; since these mutants showed WT-like ATP-driven proton pumping ability, their membrane vesicles should maintain integrity.

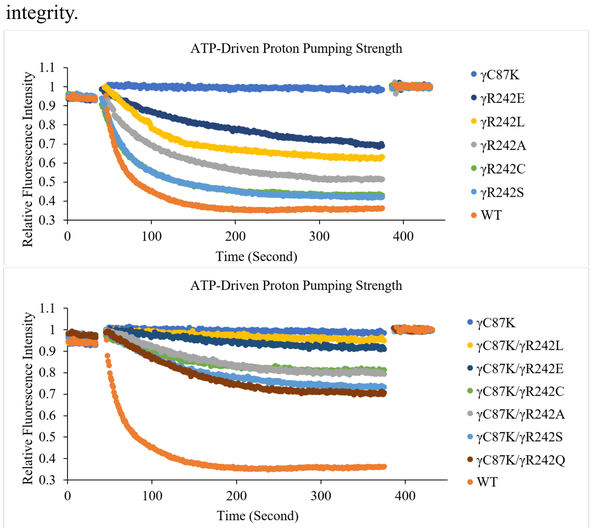

Fig. 2 Proton gradient formation ability of WT or mutant ATP synthase. The quenching of the fluorescence signal reflects the establishment of a proton gradient.

2. Mutations at γC87 and γR242 alter thermodynamic parameters of the transition state.

Table 3
Transition state thermodynamic parameters of γC87 and γR242 mutants.

Strain	$\Delta H^{\ddagger}$ kJ/mol	$T\Delta S^{\ddagger}$ kJ/mol	$\Delta G^{\ddagger}$ kJ/mol
WT	33.6 (1.7)	−37.0 (1.7)	70.6 (0.0)
Strain	**$\Delta(\Delta H^{\ddagger})$ kJ/mol**	**$\Delta(T\Delta S^{\ddagger})$ kJ/mol**	**$\Delta(\Delta G^{\ddagger})$ kJ/mol**
γC87A	−2.9 (0.5)	−2.9 (0.5)	0.0 (0.0)
γC87D	−2.3 (1.0)	−1.3 (1.0)	−1.0 (0.0)
γC87E	−2.8 (0.3)	−1.1 (0.3)	−1.7 (0.0)
γC87F	+2.9 (0.6)	+3.6 (0.6)	−0.5 (0.0)
γC87K	+19.4 (2.3)	+17.0 (2.2)	−2.4 (0.1)
γC87K/γR242A	+1.8 (2.1)	+1.4 (2.0)	+0.4 (0.1)
γC87K/γR242C	+12.8 (1.1)	+11.4 (1.1)	+1.4 (0.0)
γC87K/γR242E	+12.2 (1.2)	+10.1 (1.2)	+2.1 (0.1)
γC87K/γR242L	+32.7 (0.4)	+30.1 (0.4)	+2.7 (0.0)
γC87K/γR242Q	+8.1 (0.9)	+7.8 (0.9)	+0.3 (0.0)
γC87K/γR242S	+1.4 (1.0)	+1.1 (1.0)	+0.3 (0.0)

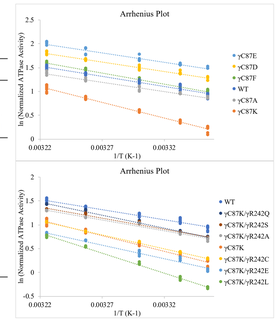

Table 3 and Fig. 3 Arrhenius analysis of membrane-bound WT or mutant ATP synthase. ATPase activity was assayed at 25 °C, 27 °C, 30 °C, 34 °C or 37 °C. Each dot in the plot shows an individual assay, and the dashed lines represent the best fit by linear regression. (A) Arrhenius analysis of γC87 mutants. (B) Arrhenius analysis of γC87K with additional γR242 mutants.

3. Molecular dynamics reveals possible residue interactions.

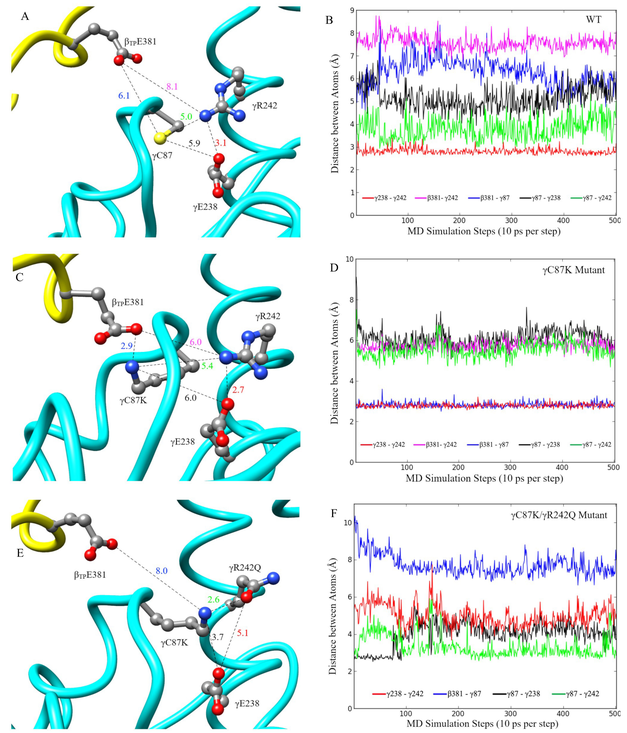

Fig. 4 Interactions of γC87 with the β_{TP}DELSEED loop. WT ATP synthase as well as γC87K and γC87K/γR242Q mutant structures were loaded for MD analysis . The last frame of each structure was illustrated by Chimera. In the Figs. A, C and E, β_{TP} and γ subunits are colored yellow and cyan respectively, and atoms are distinguished by CPK color mode (carbon element in gray, nitrogen in blue and oxygen in red). The distances between a pair of atoms are shown in Å. Figs. B, D and F show the distances between selected atoms versus the steps during MD simulations (10 ps per step).

Conclusions

1. Intra-subunit communication between γC87 and γR242 plays an important role in the energy transmission in ATP synthase.
2. Efficient energy coupling in ATP synthase relies on a cluster consisting of γC87, γM23 and $\beta_{TP/DP}$E381.

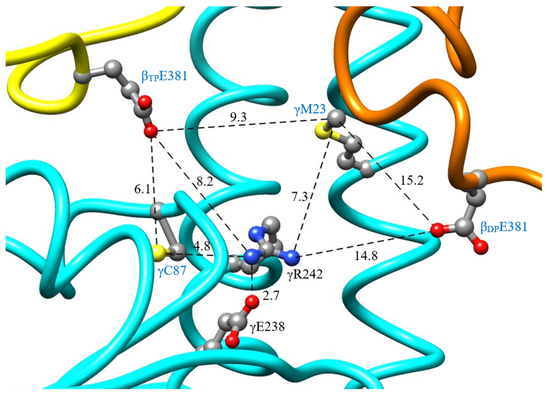

Fig. 5 Spatial relationship of residues located at the β and γ-neck interface. The figure is based on the crystal structure of *E. coli* ATP synthase (PDB ID: 3OAA). β_{TP}, β_{DP} and γ subunits are colored yellow, orange and cyan respectively. The CPK color mode is applied to distinguish different elements (carbon in gray, nitrogen in blue and oxygen in red). Distances among selected atom pairs are shown in Å. A residue labeled in blue shows that it has been reported to impair efficient energy coupling when replaced by lysine or arginine.

Grants

This work was supported in part by the Robert A. Welch Foundation (m-0200) to the department of chemistry and biochemistry, Texas Woman's University. This work was also supported in part by NIH grant GM071462 (including ARRA Administrative Supplement) to JW.

Acknowledgments

The authors would like to thank Drs. Mary E. Anderson, Richard D. Sheardy (TWU Chemistry) and Michael P. Latham (TTU Chemistry) for their many helpful discussions and kind assistance with instrumentation. The authors also acknowledge the Texas Advanced Computing Center (TACC, http://www.tacc.utexas.edu) at The University of Texas at Austin for providing the High-Performance Computing resources to this study.

References

Li, Y., Ma, X., & Weber, J. (2019). Interaction between γC87 and γR242 residues participates in energy coupling between catalysis and proton translocation in *Escherichia coli* ATP synthase. *Biochimica et Biophysica Acta - Bioenergetics*, 1860, 679–687. https://doi.org/10.1016/j.bbabio.2019.06.016